European Polymer Journal 45 (2009) 1072–1079

Contents lists available at ScienceDirect

European Polymer Journal

journal homepage: www.elsevier.com/locate/europolj

Macromolecular Nanotechnology

Controllable synthesis of nanosilica surface-grafted PMMA macromonomers via catalytic chain transfer polymerization

Zhen Lu, Jiyi Wang, Qing Li, Li Chen, Su Chen *

State Key Laboratory of Material-Oriented Chemical Engineering and College of Chemistry and Chemical Engineering, Nanjing University of Technology, No. 5 Xin Mofan Rd., Nanjing 210009, PR China

ARTICLE INFO

Article history:
Received 5 May 2008
Received in revised form 25 September 2008
Accepted 27 September 2008
Available online 19 October 2008

Keywords:
Catalytic chain transfer polymerization (CCTP)
Poly(methyl methacrylate) (PMMA)
Nanosilica
Grafting polymerization

ABSTRACT

Catalytic chain transfer polymerization (CCTP) has emerged as an efficacious method to produce low-molecular weight polymers. In this paper, we reported the first controllable synthesis of nanosilica surface-grafted poly(methyl methacrylate) (PMMA) (SI-PMMA) macromonomers by using bis(aqua)bis((difluoroboryl)-dimethylglyoximato)cobalt(II) (CoBF) as a chain transfer catalyst via CCTP. In a typical run, we firstly prepared functionalized nanosilica by using 3-(trimethoxysilyl)propylmethacrylate (MPS) as the coupling agent, allowing naosilica containing unsaturated double bonds in end groups. Subsequently, SI-PMMA macromonomers were prepared by PMMA surface-grafted onto the functionalized nanosilica via CCTP. The as-prepared products were characterized by Fourier transforms infrared (FT-IR) spectrum, thermogravimetric analysis (TGA), scanning electron microscopy (SEM), Fourier transforms Raman (FT-Raman) spectrum and gel permeation chromatography (GPC). We also investigated the dependence of macromonomers on CoBF concentrations.

1. Introduction

During the past decade, controllable fabrication of inorganic–organic polymer hybrid composites based on the molecular level has been extensively investigated due to their potential applications, such as electrochemical sensors, drug carriers and nanocomposites materials [1–7]. However, it seems to be difficult to obtain well-dispersed inorganic–organic nanocomposites owing to the strong tendency of aggregation among inorganic nanoparticles, which may serve to depress properties of nanocomposites. To this end, considerable efforts have been devoted to the design and controlled fabrication of well-defined inorganic–organic polymer hybrids. There are two principle approaches for attaching polymer chains onto surfaces of nanoparticles, involving chemisorptions [8], covalent attachment of end-functionalized polymers to a reactive surface (“grafting to”) [9] and in situ monomer polymerization with monomer growth of polymer chains from immobilized initiators (“grafting from”) [10,11]. Among these methods, the “grafting from” approach offers the most promising method in the synthesis of inorganic–organic polymer hybrids with high grafting density. Recently, several research groups have reported the synthesis of inorganic–organic polymer hybrids via “grafting from” method, such as anionic [12–15], cationic [16–18], radical [19,20], ring-opening polymerization (ROP) [21–24], atom transfer radical polymerization (ATRP) [25–29], reversible addition-fragmentation chain transfer polymerization (RAFT) [30–33] and frontal polymerization (FP) [34–39]. Dubois and co-workers [21] reported the ring-opening polymerization of ε-caprolactone initiated from amine or hydroxyl groups spreading over the surface of silica. Fukuda et al. [25] developed a useful route to the modification of silica particles by surface-initiated ATRP and synthesized hybrid nanoparticles with a monodisperse silica core and a well-defined concentrated PMMA brush. Most recently, Pan et al. [30] presented a method for preparation of RAFT agent anchored nanosilica surface, and synthesized

* Corresponding author. Tel./fax: +86 25 83587194.
E-mail address: chensu@njut.edu.cn (S. Chen).

0014-3057/$ - see front matter © 2009 Published by Elsevier Ltd.
doi:10.1016/j.eurpolymj.2008.09.042

polystyrene (PS) grafted silica particles through RAFT polymerization. Chen et al. [34,35] reported a facile method for fabrication of nanosilica–polymer nanocomposites via FP and positional assembly [40].

Although a wealth of methods have been applied on incorporating polymer onto silica surface, there are few reports on preparation of nanosilica–polymer nanocomposites by using the method of catalytic chain transfer polymerization (CCTP). CCTP has emerged as a very efficient technique for producing vinyl end-functionalized low-molecular weight polymers via free-radical polymerization [41–43], which based upon the property of certain low-spin Co(II) complexes to catalyze the chain transfer to monomer reaction. Up to now, CCTP has been only applied in the synthesis of graft or block copolymers with low-molecular weight, which can be used in a bulk or conventional emulsion process. However, the utilization of CCTP to fabricate nanosilica surface-grafted polymer macromonomers has not been described. Our preliminary works on nanosilica–polymer nanocomposites focused on how to obtain well-dispersed polymer nanocomposites by the assembly between nanosilica functionalized with low-molecular chemical agents and polymers [34,35,40,44,45]. We believe nanosilica macromonomer hybrids containing vinyl end-functionalized groups prepared by CCTP may have numerous potential applications, such as further preparation of well-defined high performance inorganic–organic network hybrids.

In the present paper, we first described the synthesis of nanosilica surface-grafted poly(methyl methacrylate) (PMMA) (SI-PMMA) macromonomers via CCTP. Since silica nanoparticles are easy to aggregate in the polymer matrix owing to their high surface area and surface energy, we firstly use 3-(trimethoxysilyl)propylmethacrylate (MPS) as the coupling agent to prepare vinyl-functionalized nanosilica. Subsequently, dangling double bonds to some extent remain on the surface of functionalized nanosilica particles, allowing them to further graft into PMMA matrix in situ. Finally, controllable synthesis of well-defined SI-PMMA macromonomers with terminal unsaturated double bond via CCTP has been successfully carried out. FT-IR, FT-Raman, TGA, SEM and GPC results of SI-PMMA macromonomers prepared by CCTP were thoroughly characterized.

2. Experimental

2.1. Materials

Methyl methacrylate (MMA) (Aldrich, 99%) was purified by the distillation under reduced vacuum to remove inhibitor. The initiator, 2,2′-azoisobutyronitrile (AIBN) (Aldrich), was purified by recrystallization from methanol. The coupling agent 3-(trimethoxysilyl)propylmethacrylate (MPS) (Aldrich) were used as received. The monomer MMA and toluene (Aldrich) were sparged with high purity nitrogen (BOC Gas) at least 2 h prior to use. Spherical silica nanoparticles (diameter = 35 nm, BET = 160 m^2, Mingri) were dried at 110 °C under vacuum for 8 h prior to use. The cobalt catalyst bis(aqua)bis((difluoroboryl)-dimethylglyoximato)-cobalt(II) (CoBF, as seen in Scheme 1) was prepared as the literature [46]. CoBF was analyzed using elemental analysis (C: 22.86%, N: 13.4%, H: 3.89%).

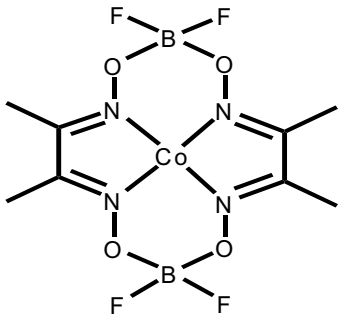

Scheme 1. Structure of cobalt catalyst CoBF.

2.2. Synthesis of MPS functionalized nanosilica (SI-MPS)

Five grams of dried spherical nanosilica (SI) was firstly dispersed in 150 g of toluene and stirred vigorously for 2 h, and then the mixture was mixed with 5.0 g MPS at 110 °C for 12 h with vigorous stirring under nitrogen. After isolation and wash with fresh toluene for five times, the free MPS was completely removed. Finally, the nanosilica functionalized with MPS (SI-MPS) containing double bonds on the surface of nanosilica, which can further polymerize with MMA monomers, were done.

2.3. Synthesis of nanosilica surface-grafted PMMA (SI-PMMA) macromonomers via CCTP

In a typical run, SI-MPS (0.6 g), AIBN (0.15 g), MMA (30 g), CoBF (0 mg, 0.13 mg, 0.38 mg, 0.63 mg, respectively) and toluene (70 g) were placed in a flask equipped with a magnetic stirrer under oxygen-free conditions by six freeze–pump–thaw cycles. The flask was consecutively evacuated and purged with nitrogen for six times. Then, the reaction mixture was placed in water bath maintaining isothermal reaction condition at 60 °C. After 1 h, the reaction was quenched in an ice bath and followed by the addition of methanol (10 mL). The products SI-PMMA macromonomers were then isolated by centrifugation and washing recycles, twice with toluene, twice with acetone and four times with toluene/acetone (1/1 v/v) mixtures. After dried under vacuum at ambient temperature overnight, the SI-PMMA macromonomers were done.

2.4. Characterization

The chemical structure of SI-PMMA macromonomers was analyzed by Fourier transform infrared (FT-IR) spectrum in the range of 400–4000 cm^{-1} using a Nicolet 6700 spectrometer (KBr disk, 64 scans, 4 cm^{-1} resolution). Fourier transforms Raman (FT-Raman) spectra were performed on a NXR FT-Raman Module by sharing interferometer installed in the FT-IR bench. The Raman optics system is comprised of Nd: YVO_4 laser operating at 1064 nm, sample holders, an InGaAs detector and a CaF_2 beam spliter.

Spectra of fine powder samples pressed in a suitable sample holder were then collected with a laser power of 1.0 W, a mirror velocity of 0.3165 cm s^{-1}, and 128 scans at a resolution of 8 cm^{-1}. The grafting percentages of SI-MPS and SI-PMMA macromonomers were determined by thermogravimetric analysis (TGA) on a Shimadzu TGA-50 with a heating rate of 10 °C/min from 38 to 700 °C. The morphology of SI-PMMA macromonomers was characterized by scanning electron microscopy (SEM) using a HITACHI-S-2150 at 15.0 kv. The samples were prepared by dispersing in toluene and applying drops of hybrids onto SEM stubs, followed by drying at ambient temperature. Molecular weight distributions were analyzed by gel permeation chromatography (GPC) using a Waters 1515 isocratic pump, a Waters 717 plus autosampler, a column set consisting of three Waters Styragel® columns (7.8 × 300 mm) HR4, HR3, HR1 and a Waters 2414 differential refractive index detector. Tetrahydrofuran (TEDIA, HPLC grade) was used as eluent at 0.6 mL/min. Calibration of the GPC equipment was carried out with narrow polystyrene standards (Shodex® Standard, peak molecular weights range 1200–538,000 g mol^{-1}).

3. Results and discussion

3.1. Synthesis of SI-PMMA macromonomers and characterization

The synthesis of SI-PMMA macromonomers involves functionalizing nanosilica and graft polymerization as described in Scheme 2. To gain complete encapsulation of silica nanoparticles with PMMA macromonomers, the amount of MPS used here was excess, ensuring the silanol groups of nanosilica to completely react with the alkoxylsilane groups of MPS. The maximum functionality of nanosilica is favorable to further obtain high-density SI-PMMA macromonomers via CCTP. Over the past two decades, CCTP of methacrylates derivatives using cobalt complexes has been now well-established as a powerful synthetic route to functionalized oligomers [47,48]. CoBF complex was demonstrated to catalyze the chain transfer to monomer reaction, producing a dead polymer chain with a terminal double bond and a monomeric radical [41]. Therefore, we can make use of this characteristic of CCTP to prepare SI-PMMA macromonomers via the graft polymerization between SI-MPS and MMA monomers. In this case, these macromonomers could contain the multi-carboxyl and terminal unsaturated carbon–carbon double bonds in polymer chains.

In order to investigate chemical structure of SI-MPS and SI-PMMA macromonomers, we use FT-IR to characterize the samples of SI-MPS and SI-PMMA macromonomer, along with the control sample for comparison (as shown in Fig. 1). Fig. 1a, b and c present the FT-IR spectra of pure nanosilica, SI-MPS and SI-PMMA macromonomer, respectively. As seen in Fig. 1a, it exhibits strong absorption peaks at 3440 cm^{-1} (Si—OH), 1110 cm^{-1} (Si—O—Si) and 810 cm^{-1} (Si—O) in the FT-IR spectrum of pure nanosilica, respectively. However, as shown in Fig. 1b and c, the absorption peak of Si—OH group in the spectra of SI-MPS and SI-PMMA becomes weaker, respectively, since hydroxyl groups on the surface of nanosilica have been partially reacted with methoxy group of MPS via condensation reaction. Also, Fig. 1b shows that there are new absorption peaks in the spectrum of SI-MPS appeared at 1700 cm^{-1} (C=O) and 2920 cm^{-1} (CH_2), respectively, indicating that the functionalized nanosilica contains the acrylate group after MPS modification. Comparing Fig. 1b with c, we have found that the absorption peaks in the spectrum of SI-PMMA macromonmer occurred at 1730 cm^{-1} (C=O) and 2950 cm^{-1} (CH_2) become stronger than those in the spectrum of SI-MPS, correspondingly, which may attribute to the formation of the nanosilica surface-grafted PMMA.

The grafting percentages of SI-MPS and SI-PMMA macromonomer were determined by TGA measurement under a nitrogen atmosphere. In order to obtain exact results of TGA, all the samples were washed and isolated completely for several times, allowing free MPS or free PMMA homopolymers to be completely removed. Fig. 2 presents the TGA curves of SI-MPS and SI-PMMA

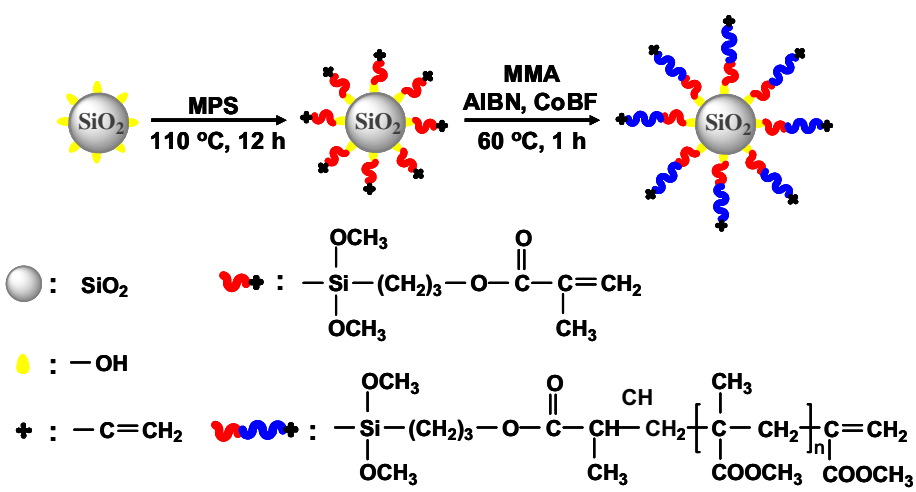

Scheme2. Schematic formation of SI-PMMA macromonomers.

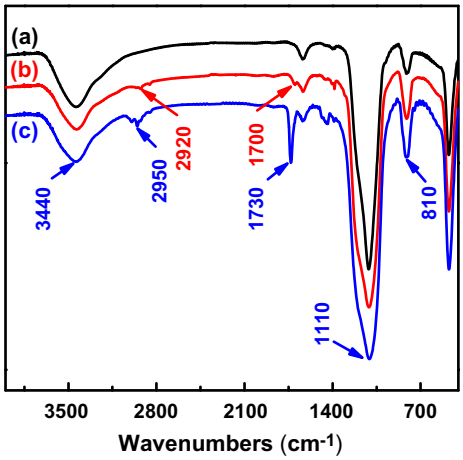

Fig. 1. FT-IR spectra of (a) pure nanosilica, (b) SI-MPS, MPS/nanosilica = 1/1 wt%; nanosilica wt% = 3 wt%; solvent, toluene; reaction time, 12 h; (c) SI-PMMA macromonomers, SI-MPS wt% = 0.6 wt%; MMA wt% = 30 wt%; AIBN/MMA = 0.5 wt%; [CoBF]/[MMA] = 3.0×10^{-6} mol mol^{-1}; solvent, toluene; reaction time, 1 h.

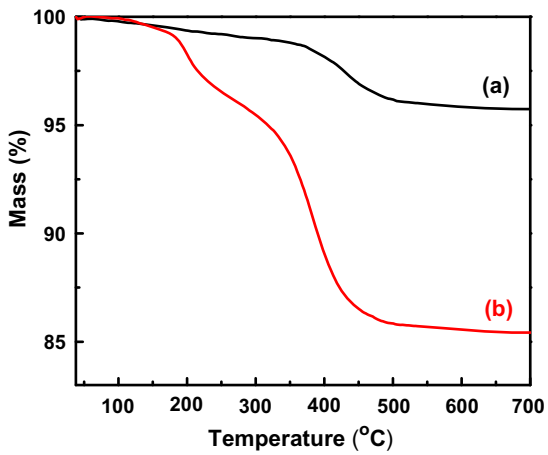

Fig. 2. TGA curves of (a) SI-MPS, MPS/nanosilica = 1/1 wt%; nanosilica wt% = 3 wt%; solvent, toluene; reaction time, 12 h; (b) SI-PMMA macromonomers, SI-MPS wt% = 0.6 wt%; MMA wt% = 30 wt%; AIBN/MMA = 0.5 wt%; [CoBF]/[MMA] = 3.0×10^{-6} mol mol^{-1}; solvent, toluene; reaction time, 1 h.

macromonomers. As shown in Fig. 2, the weight losses of SI-MPS and SI-PMMA macromonomer are 4.2% and 14.6%, respectively. According to following Eq. (1) [49], the individual grafting percentages of SI-MPS and SI-PMMA macromonomer are 4.4% and 17.1%, respectively. These TGA results are in good agreement with the FT-IR spectra results, showing that MPS and PMMA macromonomer chains have been successfully grafted onto the surface of nanosilica.

$$\text{Percentage of grafting } (\%) = \frac{\text{polymer-grafted (g)}}{\text{silica used (g)}} \times 100\% \quad (1)$$

High resolution SEM is employed to investigate the surface morphology of SI-PMMA macromonomer. Fig. 3a and b present SEM images of SI-PMMA macromonomer with low-magnification and high-magnification, respectively. It can be observed that nanoparticles of SI-PMMA macromonomer presents well-uniform and narrow distribution without any aggregation, and the average particle size of SI-PMMA macromonomer is about 40 nm. Typically, silica nanoparticles have high surface area and surface energy, and are easy to aggregate in the polymer matrix. After PMMA grafting onto the surface of nanosilica via CCTP technique, the structure of SI-PMMA macromonomer may present core–shell structure, allowing particles of SI-PMMA macromonomer to behave well-dispersed and uniform without aggregation.

In order to gain an insight into the process of MMA monomers grafting onto the surface of nanosilica via CCTP, we measured FT-Raman spectra in the region of 1000–3500 cm^{-1} for the sample of free PMMA homopolymers produced during the synthesis of SI-PMMA macromonomer via CCTP (seen in Fig. 4b), along with the control sample via free-radical polymerization for comparison (seen in Fig. 4a). In comparison Fig. 4a with b, most of characteristic peaks are similar, such as they all exhibit the characteristic peaks at 1450 cm^{-1} (CH_2 deformation vibration), 2850 cm^{-1} (CH_2 stretching vibration), 2950 cm^{-1} and 3000 cm^{-1} (CH_3 asymmetry stretching vibration), 1730 cm^{-1} (C=O in the ester carbonyl group), respectively. For the distinct difference between Fig. 4a and b, there is new characteristic peak appeared at 1630 cm^{-1} in Fig. 4b, which is attributed to the characteristic peak of C=C stretching vibration. It can be explained by that the as-prepared polymers via CCTP contain a vinyl end-functionalized groups in the polymer chains. This result also indicates that the as-prepared polymers with vinyl end-functionalized PMMA chains are successfully prepared via CCTP.

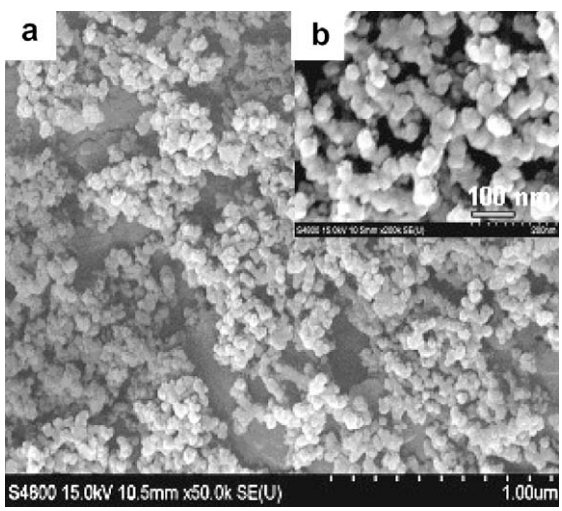

Fig. 3. High resolution SEM images of SI-PMMA macromonomers. (a) Low-magnification and (b) high-magnification, SI-MPS wt% = 0.6 wt%; MMA wt% = 30 wt%; AIBN/MMA = 0.5 wt%; [CoBF]/[MMA] = 3.0×10^{-6} mol mol^{-1}; solvent, toluene; reaction time, 1 h.

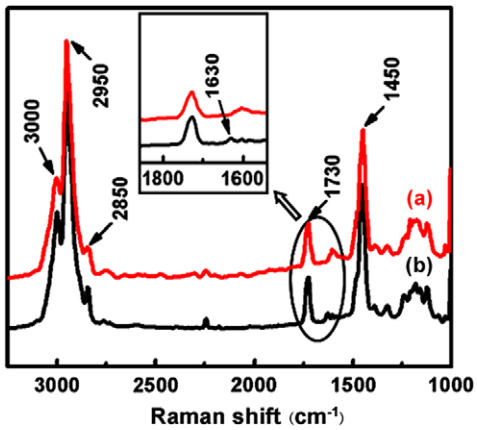

Fig. 4. FT-Raman spectra of free PMMA homopolymers produced during the synthesis of SI-PMMA macromonomers. (a) SI-MPS wt% = 0.6 wt%; MMA wt% = 30 wt%; AIBN/MMA = 0.5 wt%; solvent, toluene; reaction time,1 h; (b) SI-MPS wt% = 0.6 wt%;MMA wt% = 30 wt%; AIBN/MMA = 0.5 wt%; [CoBF]/[MMA] = 3.0×10^{-6} mol mol^{-1}; solvent, toluene; reaction time, 1 h.

3.2. Effects of the CoBF complex concentrations on CCTP

The Co(II) complexes act as very efficient catalysts for the chain transfer to monomer reaction and only ppm quantities of these catalysts are requited to obtain significant molecular weight reduction. In this study, we use BF_2-bridged cobaloximes CoBF as the catalyst to carry out CCTP. To investigate effects of CoBF concentrations on CCTP, different molar ratios of CoBF/MMA were performed in the synthetic process of PMMA grafting onto the surface of nanosilica. Fig. 5 presents FT-IR spectra of SI-PMMA macromonomer samples with different CoBF concentrations. As shown in Fig. 5, characteristic absorption peaks appeared at 1730 cm^{-1} (C=O), 2920 cm^{-1} and 1440 cm^{-1} (CH_2), 2970 cm^{-1} and 2850 cm^{-1} (CH_3) are clearly observed, respectively. Also, we have found that the strength of these characteristic absorption peaks is decreased with higher concentration of CoBF. This may be attributed to the result that the molecular weight and/or the grafting degree of SI-PMMA macromonomer are decreased with the increase of CoBF concentrations.

The TGA curves of SI-PMMA macromonomer samples prepared with different CoBF concentrations are shown in Fig. 6. As seen in Fig. 6, there are two main degradation steps in TGA curves of SI-PMMA macromonomer samples. It may be caused by that the as-prepared products prepared by CCTP exist the non-uniform of molecular weigh distributions. Also, it can be barely seen that the grafting degrees of SI-PMMA macromonomers are changed from the range of 20.9–11.6% with varying CoBF/MMA molar ratios from 0 to 5.0×10^{-6}. This result is also in good agreement with the FT-IR spectra results of SI-PMMA macromonomers as shown in Fig. 5.

For CCTP technique, it not only can produce vinyl end-functionalized polymers, but also can prepare different low-molecular weight macromonomers. Fig. 7 shows typical molecular weight distributions of free PMMA homopolymers prepared during the synthesis of SI-PMMA macromonomers with different concentrations of CoBF. A shift of the distributions towards lower molecular weights at higher CoBF concentrations can be clearly seen. As shown in Table 1, in the absence of CoBF, the number average molecular weight ($\overline{M}_n$) of free PMMA homopolymer is 7.72×10^4 g mol^{-1}. However, with the addition of CoBF, the $\overline{M}_n$ data of free PMMA homopolymers are linearly de-

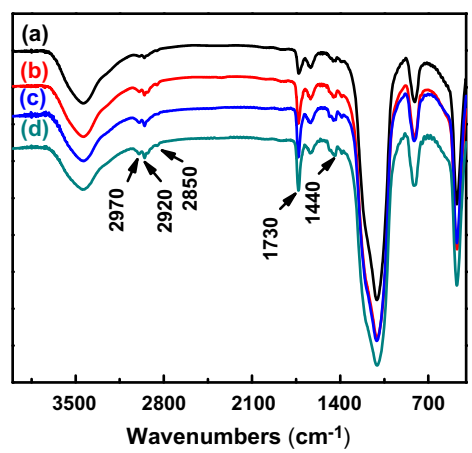

Fig. 5. FT-IR spectra of SI-PMMA macromonomers prepared with different CoBF concentrations. (a) SI-MPS wt% = 0.6 wt%; MMA wt% = 30 wt%; AIBN/MMA = 0.5 wt%; [CoBF]/[MMA] = 5.0×10^{-6} mol mol^{-1}; solvent, toluene; reaction time, 1 h; (b) SI-MPS wt% = 0.6 wt%; MMA wt% = 30 wt%; AIBN/MMA = 0.5 wt%; [CoBF]/[MMA] = 3.0×10^{-6} mol mol^{-1}; solvent, toluene; reaction time, 1 h; (c) SI-MPS wt% = 0.6 wt%; MMA wt% = 30 wt%; AIBN/MMA = 0.5 wt%; [CoBF]/[MMA] = 1.0×10^{-6} mol mol^{-1}; solvent, toluene; reaction time, 1 h; (d) SI-MPS wt% = 0.6 wt%; MMA wt% = 30 wt%; AIBN/MMA = 0.5 wt%; solvent, toluene; reaction time, 1 h.

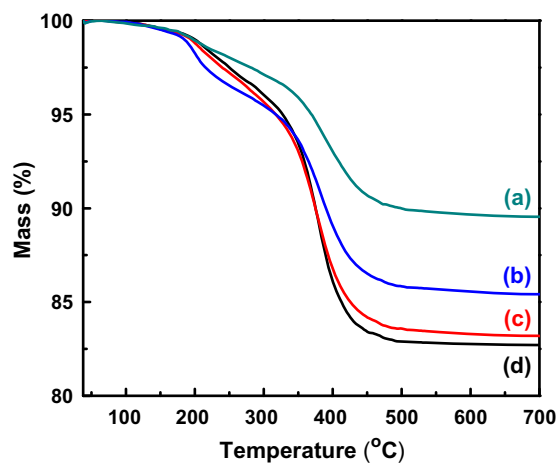

Fig. 6. TGA curves of SI-PMMA macromonomers prepared with different CoBF concentrations. (a) SI-MPS wt% = 0.6 wt%; MMA wt% = 30 wt%; AIBN/MMA = 0.5 wt%; [CoBF]/[MMA] = 5.0×10^{-6} mol mol^{-1}; solvent, toluene; reaction time, 1 h; (b) SI-MPS wt% = 0.6 wt%; MMA wt% = 30 wt%; AIBN/MMA = 0.5 wt%; [CoBF]/[MMA] = 3.0×10^{-6} mol mol^{-1}; solvent, toluene; reaction time, 1 h; (c) SI-MPS wt% = 0.6 wt%; MMA wt% = 30 wt%; AIBN/MMA = 0.5 wt%; [CoBF]/[MMA] = 1.0×10^{-6} mol mol^{-1}; solvent, toluene; reaction time, 1 h; (d) SI-MPS wt% = 0.6 wt%; MMA wt% = 30 wt%; AIBN/MMA = 0.5 wt%; solvent, toluene; reaction time, 1 h.

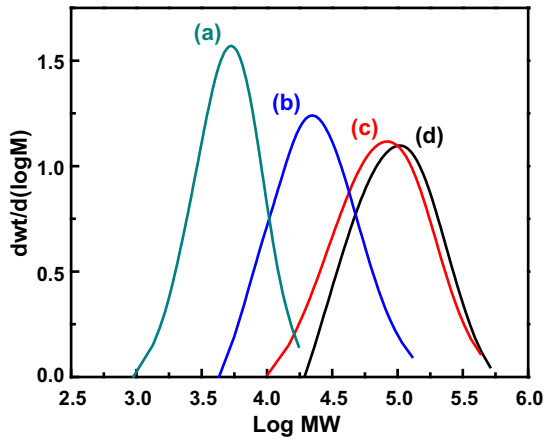

Fig. 7. Molecular weight distributions of free PMMA homopolymers produced during the synthesis of SI-PMMA macromonomers with different CoBF concentrations. (a) SI-MPS wt% = 0.6 wt%; MMA wt% = 30 wt%; AIBN/MMA = 0.5 wt%; [CoBF]/[MMA] = 5.0×10^{-6} mol mol^{-1}; solvent, toluene; reaction time, 1 h; (b) SI-MPS wt% = 0.6 wt%; MMA wt% = 30 wt%; AIBN/MMA = 0.5 wt%; [CoBF]/[MMA] = 3.0×10^{-6} mol mol^{-1}; solvent, toluene; reaction time, 1 h; (c) SI-MPS wt% = 0.6 wt%; MMA wt% = 30 wt%; AIBN/MMA = 0.5 wt%; [CoBF]/[MMA] = 1.0×10^{-6} mol mol^{-1}; solvent, toluene; reaction time, 1 h; (d) SI-MPS wt% = 0.6 wt%; MMA wt% = 30 wt%; AIBN/MMA = 0.5 wt%; solvent, toluene; reaction time, 1 h.

Table 1
Molecular weights and PDI data of free PMMA homopolymers prepared during the synthesis of SI-PMMA macromonomers with different CoBF concentrations via CCTP.

[CoBF]/[MMA]/(mol mol^{-1})	$\overline{M}_n$/(g mol^{-1})	$\overline{M}_w$/(g mol^{-1})	PDI
0	77219	129220	1.673
1.0×10^{-6}	57826	96569	1.670
3.0×10^{-6}	18550	30747	1.658
5.0×10^{-6}	4211	5833	1.390

creased from 57826 to 4211 g mol^{-1} corresponding with varying CoBF/MMA molar ratios from 1.0×10^{-6} to 5.0×10^{-6}, respectively. Additionally, similar trend of polydispersity index (PDI) of free PMMA homopolymers can be clearly observed. It also indicates that the molecular weight distributions of free PMMA homopolymers become narrower with higher concentration of CoBF.

3.3. The mechanism on synthesis of SI-PMMA macromonomers via CCTP

The assumed mechanism on synthesis of SI-PMMA macromonomers via CCTP is shown in Scheme 3. In catalytic chain transfer polymerization, initiation, propagation and termination are thought to occur by a free-radical process [41–43]. The Co(II) complex abstracts a hydrogen atom from the polymeric radical on the surface of vinyl-functionalized nanosilica, resulting in the formation of dead PMMA chain with terminal unsaturated double bond and a Co(III)–H complex. This Co(III)–H complex is very reactive and can react with a MMA monomer molecule by a hydrogen transfer reaction, resulting in a monomeric radical and the regeneration of the original Co(II) catalyst. As a result, when increasing the concentration of CoBF, the tendency for Co(II) complex abstracting hydrogen atoms from polymeric radical is intensified. It may further restrain the process of polymer chain propagation, thus leading to the reduction of the grafting degree and molecular weight of PMMA grafted onto the surface of nanosilica. These deduce was also confirmed by the results of FT-IR, TGA and GPC.

4. Conclusions

A new available strategy for fabricating nanosilica surface-grafted PMMA macromonomers via CCTP technique has been successfully achieved. Firstly, we employed MPS as the coupling agent to prepare vinyl-functionalized nanosilica. Subsequently, dangling double bonds to some extent remain on the surface of functionalized nanosilica particles, allowing them to further graft with PMMA macromonomers via CCTP in situ. Finally, controllable syn-

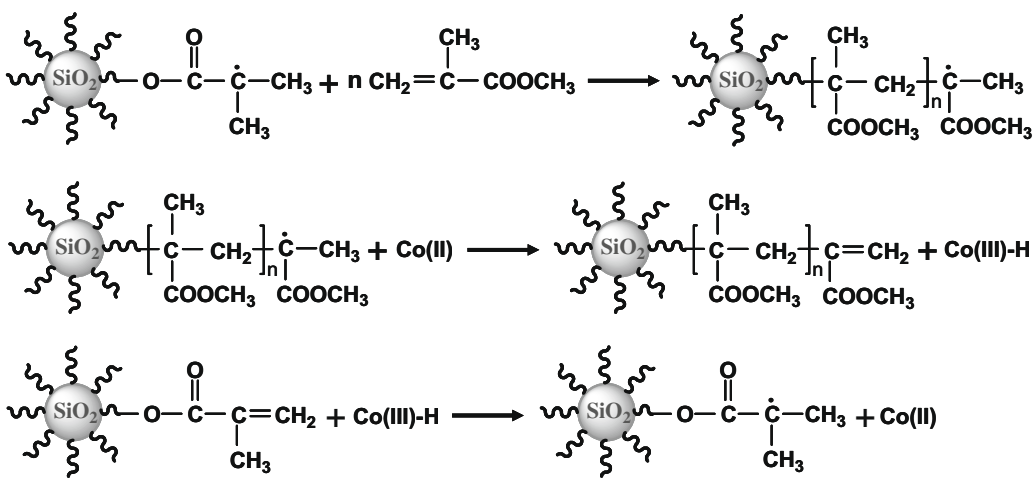

Scheme 3. The assumed mechanism on synthesis of SI-PMMA macromonomers via CCTP.

thesis of well-defined nanosilica surface-grafted PMMA macromonomers with terminal unsaturated double bond has been produced via CCTP.

A thorough study on the effects of the CoBF complex concentrations on the grafting degree of SI-PMMA macromonomer and molecular weights of free PMMA homopolymers prepared during the synthetic process of nanosilica surface-grafted PMMA was performed. We can control the molecular weights of PMMA macromonomer chains through adding proper amount of CoBF complexes. The FT-IR, TGA and SEM results indicate that PMMA macromonomers have been successfully tethered onto the surface of nanosilica. The FT-Raman spectra show that PMMA macromonomer chains are terminated with vinyl groups. Moreover, GPC results indicate that molecular weights of free PMMA homopolymers prepared during the synthetic process of nanosilica surface-grafted PMMA macromonomers dramatically decreases with an increase of CoBF complex concentration. This similar trend from TGA results of SI-PMMA macromonomers can be drawn. The assumed mechanism on nanosilica surface-grafted PMMA macromonomers may gain an insight into the process of MMA monomers grafting onto the surface of nanosilica via CCTP. A parallel approaches to that of this investigation constitutes a promising way to fabricate inorganic–organic macromonomers via CCTP technique may follow.

Acknowledgements

This work was supported by the National Natural Science Foundation of China (Grant Nos. 20576053, 20606016), NASA (Grant No. 10676013), and the Natural Science Foundation of the Jiangsu Higher Education Institutions of China (Grant No. 07KJA53009).

References

[1] Alain W. Electrochemical applications of silica-based organic–inorganic hybrid materials. Chem Mater 2001;13(10):3351–72.
[2] Guo J, Yang WY, Wang CC, He J, Chen JY. Poly(*N*-isopropylacrylamide)-coated luminescent/magnetic silica microspheres: preparation, characterization, and biomedical applications. Chem Mater 2006;18(23):5554–62.
[3] Sertchook H, Elimelech H, Makarov C, Khalfin R, Cohen Y, Shuster M, et al. Composite particles of polyethylene at silica. J Am Chem Soc 2007;129(1):98–108.
[4] Chen L, Zhu J, Li Q, Chun S, Wang YR. Controllable synthesis of functionalized CdS nanocrystals and CdS/PMMA nanocomposite hybrids. Eur Polym J 2007;43(11):4593–601.
[5] Chen S, Zhu J, Shen YF, Hu CH, Chen L. Synthesis of nanocrystal-polymer transparent hybrids via polyurethane matrix grafted onto functionalized CdS nanocrystals. Langmuir 2007;23(2):850–4.
[6] Guo L, Chen S, Chen L. Controllable synthesis of ZnS/PMMA nanocomposite hybrids generated from functionalized ZnS quantum dots nanocrystals. Colloid Polym Sci 2007;285(14):1593–600.
[7] Zelazowska E, Borczuch-Laczka M, Rysiakiewicz-Pasek E. Sol–gel derived organic–inorganic hybrid electrolytes for thin film electrochromic devices. J Non Cryst Solids 2007;353(18–21):2104–8.
[8] Pyun J, Matyjaszewski K. Synthesis of nanocomposite organic/inorganic hybrid materials using controlled/"living" radical polymerization. Chem Mater 2001;13(10):3436–48.
[9] Vonwerne T, Paatten EP. Atom transfer radical polymerization from nanoparticles: a tool for the preparation of well-defined hybrid nanostructures and for understanding the chemistry of controlled/"living" radical polymerizations from surfaces. J Am Chem Soc 2001;123(31):7497–505.
[10] Vonwerne T, Paatten EP. Preparation of structurally well-defined polymer-nanoparticle hybrids with controlled/living radical polymerizations. J Am Chem Soc 1999;121(32):7409–10.
[11] Spange S. Silica surface modification by cationic polymerization and carbenium intermediates. Prog Polym Sci 2000;25(6):781–849.
[12] Zhou Q, Wang S, Fan X, Advincula R, Mays J. Living anionic surface-initiated polymerization (LASIP) of a polymer on silica nanoparticles. Langmuir 2002;18(8):3324–31.
[13] Jordan R, Ulman A, Kang JF, Rafailovich MH, Sokolov J. Surface-initiated anionic polymerization of styrene by means of self-assembled monolayers. J Am Chem Soc 1999;121(5):1016–22.
[14] Jordan R, Ulman A. Surface initiated living cationic polymerization of 2-oxazolines. J Am Chem Soc 1998;120(2):243–7.
[15] Samoshina Y, Diaz A, Becker Y, Nylander T, Lindamana B. Adsorption of cationic, anionic and hydrophobically modified polyacrylamides on silica surfaces. Colloid Surf A Physicochem Eng Asp 2003;231(1–3):195–205.
[16] Luna-Xavier JL, Guyot A, Bourgeat-Lamil E. Synthesis and characterization of silica/poly (methyl methacrylate) nanocomposite latex particles through emulsion polymerization using a cationic azo initiator. J Colloid Interface Sci 2002;250(1):82–92.
[17] Spange S, Meyer T. Cationic surface polymerization of 1,3-divinylimidazolid-2-one for immobilization on silica gel particles. Macromol Chem Phys 1999;200(7):1655–61.
[18] Zhao B, Brittain WJ, Zhou WS, Cheng SZD. Nanopattern formation from tethered PS-*b*-PMMA brushes upon treatment with selective solvents. J Am Chem Soc 2000;122(10):2407–8.
[19] Meyer T, Spange S, Hesse S, Jager C, Bellmann C. Radical grafting polymerization of vinylformamide with functionalized silica particles. Macromol Chem Phys 2003;204(4):725–32.
[20] Ueda J, Sato S, Tsunokawa A, Yamauchi T, Tsubokawa N. Scale-up synthesis of vinyl polymer-grafted nano-sized silica by radical polymerization of vinyl monomers initiated by surface initiating groups in the solvent-free dry-system. Eur Polym J 2005;41(2):193–200.
[21] Carrot G, Rutot-Houze D, Pottier A, Degee P, Hilborn J, Dubois P. Surface-initiated ring-opening polymerization: a versatile method for nanoparticle ordering. Macromolecules 2002;35(22):8400–4.
[22] Lahann J, Langer R. Surface-initiated ring-opening polymerization of ε-caprolactone from a patterned poly(hydroxymethyl-*p*-xylylene). Macromol Rapid Commun 2001;22(12):968–71.
[23] Juang A, Scherman OA, Grubbs RH, Lewis NS. Formation of covalently attached polymer overlayers on Si(111) surfaces using ring-opening metathesis polymerization methods. Langmuir 2001;17(5):1321–3.
[24] Yoshinaga K, Fujiwara K, Mouri E, Ishii M, Nakamura H. Stepwise controlled immobilization of colloidal crystals formed by polymer-grafted silica particles. Langmuir 2005;21(10):4471–7.
[25] Ohno K, Morinaga T, Koh K, Tsujii Y, Fukuda T. Synthesis of monodisperse silica particles coated with well-defined, high-density polymer brushes by surface-initiated atom transfer radical polymerization. Macromolecules 2005;38(6):2137–42.
[26] Lei ZL, Bi SX. Preparation of polymer nanocomposites of core–shell structure via surface-initiated atom transfer radical polymerization. Mater Lett 2007;61(16):3531–4.
[27] Morinaga T, Ohkura M, Ohno K, Tsujii Y, Fukuda T. Monodisperse silica particles grafted with concentrated oxetane-carrying polymer brushes: their synthesis by surface-initiated atom transfer radical polymerization and use for fabrication of hollow spheres. Macromolecules 2007;40(4):1159–64.
[28] Zhao HY, Kang XL, Liu L. Comb-coil polymer brushes on the surface of silica nanoparticles. Macromolecules 2005;38(26):10619–22.
[29] Harrak E, Carrot G, Oberdisse J, Jestin J, Boue F. Atom transfer radical polymerization from silica nanoparticles using the 'grafting from' method and structural study via small-angle neutron scattering. Polymer 2005;46(4):1095–104.
[30] Hong CY, Li X, Pan CY. Grafting polymer nanoshell onto the exterior surface of mesoporous silica nanoparticles via surface reversible addition-fragmentation chain transfer polymerization. Eur Polym J 2007;43(10):4114–22.
[31] Liu CH, Pan CY. Grafting polystyrene onto silica nanoparticles via RAFT polymerization. Polymer 2007;48(13):3679–85.
[32] Li CZ, Han J, Ryu CY, Benicewicz BC. A versatile method to prepare RAFT agent anchored substrates and the preparation of PMMA grafted nanoparticles. Macromolecules 2006;39(9):3175–83.
[33] Li CZ, Benicewicz BC. Synthesis of well-defined polymer brushes grafted onto silica nanoparticles via surface reversible addition-fragmentation chain transfer polymerization. Macromolecules 2005;38(14):5929–36.

[34] Chen L, Hu T, Yu H, Chen S, Pojman JA. First solvent-free synthesis of poly(*N*-methylolacrylamide) via frontal free-radical polymerization. J Polym Sci Part A Polym Chem 2007;45(18):4322–30.
[35] Chen S, Sui JJ, Chen L, Pojman JA. Polyurethane-nanosilica hybrid nanocomposites synthesized by frontal polymerization. J Polym Sci Part A Polym Chem 2005;43(8):1670–80.
[36] Chen S, Hu T, Tian Y, Chen L, Pojman JA. Facile synthesis of poly(hydroxyethyl acrylate) by frontal free-radical polymerization . J Polym Sci Part A Polym Chem 2007;45(5):873–81.
[37] Hu T, Fang Y, Yu H, Chen L, Chen S. Synthesis of poly(*N*-methylolacrylamide)/polymethylacrylamide hybrids via frontal free-radical polymerization. Colloid Polym Sci 2007;285(8):891–8.
[38] Hu T, Chen S, Tian Y, Pojman JA, Chen L. Frontal free-radical copolymerization of urethane-acrylates. J Polym Sci Part A Polym Chem 2006;44(9):3018–24.
[39] Chen S, Sui JJ, Chen L. Segmented polyurethane synthesized by frontal polymerization. Colloid Polym Sci 2005;283(8):932–6.
[40] Chen S, Sui JJ, Chen L. Positional assembly of hybrid polyurethane nanocomposites via incorporation of inorganic building blocks into organic polymer. Colloid Polym Sci 2004;283(1):66–73.
[41] Gridney AA, Ittel SD. Catalytic chain transfer in free-radical polymerizations. Chem Rev 2001;101(12):3611–60.
[42] Heuts JPA, Roberts BG, Biasutti JD. Catalytic chain transfer polymerization: an overview. Aust J Chem 2002;55(7):381–98.
[43] Kukulja D, Davis TP. Mechanism of catalytic chain transfer in the free-radical polymerisation of methyl methacrylate and styrene. Macromol Chem Phys 1998;199(8):1697–708.
[44] Yang SY, Chen S, Tian Y, Feng C, Chen L. Facile transformation of a native polystyrene (PS) film into a stable superhydrophobic surface via sol–gel process. Chem Mater 2008;20(4):1233–5.
[45] Chen L, Shen HX, Lu Z, Feng C, Chen S. Fabrication and characterization of TiO_2–SiO_2 composite nanoparticles and polyurethane/(TiO_2–SiO_2). Colloid Polym Sci 2007;285(13):1515–20.
[46] Bakac A, Espenson JH. Unimolecular and bimolecular homolytic reactions of organochromium and organocobalt complexes. Kinetics and equilibria. J Am Chem Soc 1984;106(18):5197–202.
[47] Gridnev A. The 25th anniversary of catalytic chain transfer. J Polym Sci Part A Polym Chem 2000;38(10):1753–66.
[48] Davis TP, Zammit MD, Heuts JPA, Moody K. A novel route to the preparation of aldehyde end-functionalised oligomers via catalytic chain transfer polymerization. Chem Commun 1998;21:2383–4.
[49] Tsubokawa N, Fujiki K, Sone Y. Radical grafting from carbon black. Graft polymerization of vinyl monomers initiated by peroxyester groups introduced onto carbon black surface. Polym J 1988;20(3):213–20.